AIRBAG-IGNITERS: LIFETIME TESTING OF BRIDGE WIRES UNDER ALTERNATING LOADS

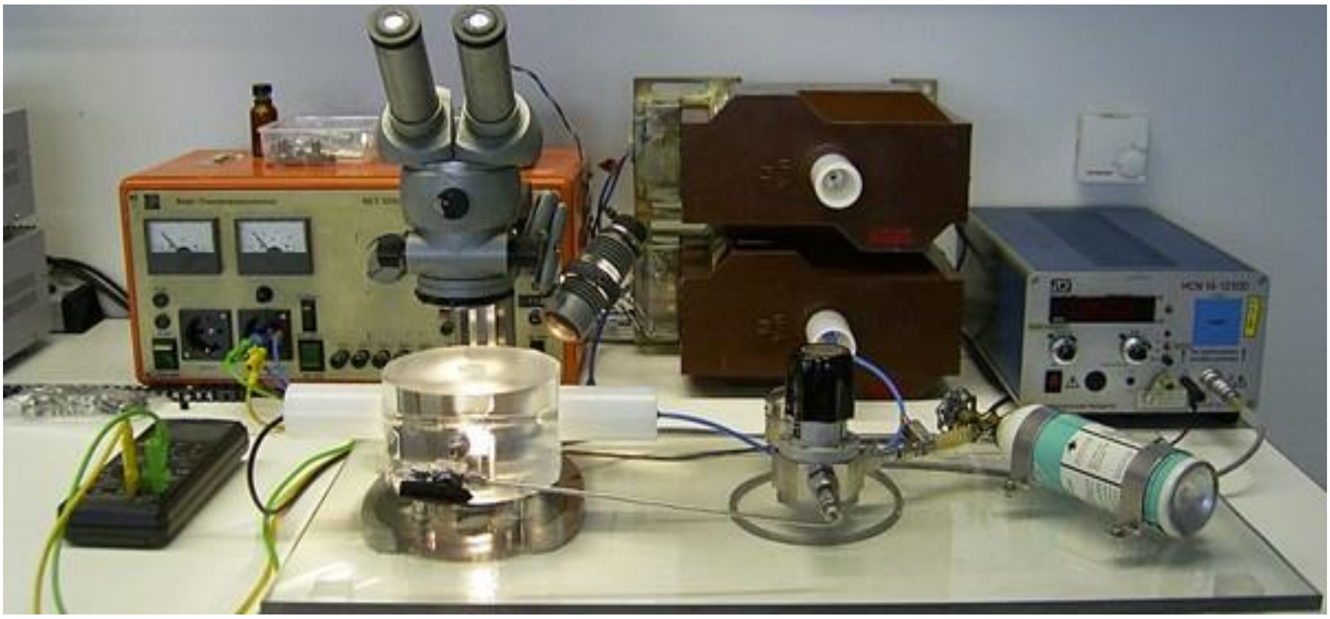

- KNOWLEDGE CREATES PROGRESS®
- **GWP WHITE PAPER ANALYTIKUM 006**
- AUTHORS

Dr. Julius Nickl
Dipl. Chemiker
Geschäftsführer
Senior-Experte
julius.nickl@gwp.eu

1 SUMMARY

The failures caused by broken ignition wires in airbag igniters prompted the development of a method for determining the mechanical strength of exposed ignition wires. The joined, but pyrotechnically free igniters were chosen as the object of investigation in order to be able to carry out fatigue vibration tests on these components.

Three methods for alternating loading of the thin wires were experimentally tested for their feasibility. The power transmission was carried out by means of:

- Magnetic fields in the passage of current
- Alternating electric fields (high voltage)
- Fluids: flowing liquid or air

In this 5-month study, concepts and their experimental implementation were tested. Only with inflows could fractures be reliably produced, so further work - with more resources - should be continued with flowing fluids.

CONTENT

2 TASK

Threshold loads on components are a major technical problem. Especially with small structures, such as here in the area of very fine wires (a few μ m in diameter), it is difficult to make statements about the durability of the processed products (also in the electronics industry). A critical point is the connection of a fully or partially movable wire with a rigid substrate. Temperature changes and vibrations generate high stresses at the joints, which can lead to fatigue and ultimately to the destruction of the component. Particularly in the automotive industry, the durability/life of safety-relevant products are considered at a very early stage. The question of the reliability of the ignition devices in airbags gave rise to the design of a test device.

3 STATE OF THE ART

3.1 Thin wires in industry

3.1.1 Existing application

By far the largest customer is the electronics industry, which uses wire conductors in the form of bridges (by insulator or free). Another important field of application are ignition wires for pyrotechnics. In micro wire erosion, the smallest components are manufactured primarily for medical applications. They are also used in measurement technology as heat sensors or as springs.

3.1.2 Materials

Because of their good conductivity, copper, aluminium and gold are mainly used in electronics. At a great distance follow nickel-chromium, and various platinum alloys, these mainly used in metrology. In addition, materials such as constantan, brass, palladium and tungsten are also available from manufacturers today.

3.1.3 Manufacture

The requirements for the material are:

- Favourable mechanical properties for small cross-sections
- Good metallurgical behaviour
- Defined electrical conductivity
- Joinability

The wire is brought from a casting in up to 50 steps to the desired cross-section. In order to avoid strain hardening, the wire is heat treated between the drawing processes. Another process is hydrostatic extrusion. This achieves large cross-section reductions with a homogeneous structure of the wire. The combined heat/drawing treatment allows the grain size to be adjusted and thus also the mechanical and, to a certain extent, the electrical behavior to be influenced.

3.2 Joining method for thin wires

The connections must meet different requirements, so there are different procedures depending on the intended use.

3.2.1 Bonding

One of the most commonly used joining techniques. Ultrasonic bonding (US welding) is often also called wedge bonding because of the mostly wedge-shaped bonding tool. The bonding tool swings parallel to the surface and applies the wire under pressure. The friction causes disturbing surface layers to crack and the roughness to be reduced. This causes wire and joining surface to approach each other up to atomic distance and connect. In
the thermocompression process, the joining partners are pressed together under heat. The compound is formed by atomic bonding forces and diffusion. There is no molten phase. The thermosonic process is a mixture of thermocompression and ultrasonic bonding.

3.2.2 Soldering (welding)

Solder joints have good conductivity, but carry the risk of embrittlement at the joint due to structural changes. The process temperatures are easily adjustable and range from 50 to 350°C depending on the solder.

3.2.3 Eutectic connections

The eutectic connection is similar to a solder joint. With a defined composition of the substances to be joined, a low-melting, eutectic alloy is formed. No connecting materials are required that may interfere with the process. High process temperatures are achieved during joining. The joint is mechanically stable and has good electrical conductivity.

3.2.4 Clamps

A large-area connection with the wire is created, therefore the connection has a good conductivity. There is a risk of damaging the wire during clamping and thus reducing the mechanical load capacity.

3.2.5 Gluing

Bonding compensates for tension differences between the substrate and the bonded material. Can also be electrically conductive, although not as good as metallic connections. Adhesives with up to 70% silver content are used for this purpose. Joining can take place at low temperatures. The operating temperatures depend on the polymer used, but are usually lower than those of the other joining methods.

3.3 Test methods

3.3.1 Optical

Under the microscope, cracks, wire breaks and unintentional deformations, such as kinks, can be detected. Due to the shape of the joint, a statement can be made about the quality of the bond connection. Cracks and fractures must be wider than the resolution limit of the microscope. It is easy to overlook mistakes because you have to look in the right direction at the right place.

3.3.2 Tensile test

In the mechanical tensile test, a hook is attached to the wire and pulled upwards at a constant speed to determine the breaking load. The location of the fracture is important for the evaluation (in the wire, transition to the welding point or welding point itself). If the joining surface is much larger than the cross-sectional area of the wire (e.g. nailhead bonding), the strength of the wire rather than that of the weld is measured.

3.3.3 Shear test

Only the joint is tested in the shear test. A shearing tool is used to apply a load to the side of the joint. The force and location of the break provide information about the quality of the connection. With a good connection the joint is sheared off, with a bad one it separates from the subsoil.

3.4 Fatigue strength of igniters

3.4.1 Diffusion

At the transition between two metals atoms can diffuse. A distinction is made between volume diffusion and grain boundary diffusion.
During volume diffusion, atoms migrate by jumping onto neighbouring empty spaces in the lattice. Blank condensation refers to the effect that the blank spaces accumulate at grain boundaries and create cavities. The velocity of volume diffusion is strongly dependent on temperature.
In grain boundary diffusion, grain boundaries with high defect density are used as diffusion paths. If the metals have different diffusion coefficients, porous spots form in the faster diffusing metal (Kirkendall effect). This process is hardly temperature-dependent and takes place faster with a fine crystalline structure.
These pores reduce the strength in the area of the contact points.

3.4.2 Corrosion

Corrosion dramatically reduces the load-bearing capacity. A distinction is made between chemical corrosion, where there is a direct reaction with oxygen, which accelerates as the temperature rises, and more frequent electrochemical corrosion, which requires the presence of an electrolyte. Electrochemical corrosion only occurs with metals of different electronegativity. The greater the difference, the faster the process progresses. If there is a large surface difference between the electrodes, a large current density is generated at the smaller one. If the smaller electrode is made of the more noble material, the corrosion takes place slowly, and vice versa very quickly.
Vibration crack corrosion (corrosion fatigue) occurs on components that are subjected to both dynamic and corrosive stress.

4 CONSIDERATION OF THE LOADS ON THE WIRE

4.1 Fatigue test

According to DIN 50100 - Fatigue test (terms, symbols, execution, evaluation).
The fatigue test is used to determine characteristic values for the mechanical behavior of components under continuous or frequently repeated, swelling or alternating loads.
The fatigue strength is the largest stress deflection oscillating around a given medium voltage

that a specimen can withstand infinitely often, without breakage and without impermissible deformation. It was generally observed that the number of oscillations reached, with decreasing applied stress, approaches asymptotically a fixed value (oscillation number infinite). Experience has shown that this value for metals is well approximated at 10×10^6 to 100×10^6 vibration cycles. In order to shorten the test duration, vibration cycles from 2×10^6 have also become established.

Since the stress is directly related to the deformation of the material, but cannot be calculated in this case without major technical aids, the specification of the applied load is initially limited to the specification of the deflection. The excitation of the wire should be realized by fields, since a direct mechanical excitation can hardly be realized. Inorder to obtain a reproducible result during a load test, it is difficult for measurement technology to transfer precisely defined vibrations to the component.

4.2 Loads on the wire

Depending on the design, the stresses that occur are made up of various components. A straight wire, similar to a string, is deflected evenly, resulting in tensile and bending stresses. While a wire with an arc additionally experiences a torque and thus a torsional stress is generated. In addition, the bending stress is divided into a flat and a perpendicular part.

The test samples are airbag igniters made of the following wire material: CrNi 80-20 (material no.: 2.4869). Mechanical and physical properties according to data sheet Thyssen Krupp VDM.

Clamping length: $\approx 900 \mu m$
Actual length: $\approx 950 \mu m$
Diameter: $25 \mu m$
Elevation h: $\approx 130 \mu m$

Torsion length $l_t: \approx 175 \mu m$

Permissible continuous current, $I_{eff}: 0.100 A$
E-module: $200 GPa$
elongation limit, $\sigma_{0,2}: \geq 280 MPa$
Tensile strength, $\sigma_m: \geq 650 Mpa$
Spec. electrical resistance: $1.12 \frac{\Omega mm^2}{m}$
Density, $\rho: 8.3 \cdot 10^3 \frac{Kg}{m^3}$

4.2.1 Deflection due to length change

1) Length variation

Δl can be calculated for known material properties and dimensions using Hook's law.

$$E = \frac{\sigma}{\varepsilon} \quad \varepsilon = \frac{\Delta l}{l_0}$$

Often the permissible elastic elongation of ε the material is also given in percent. l_0 corresponds to the actual length.

2) Approximation of deflection

The model assumed is a straight, tension-free, completely flexible wire of length a, in the middle of which a constant force Fmag applies. (Approximation for very small deflections)

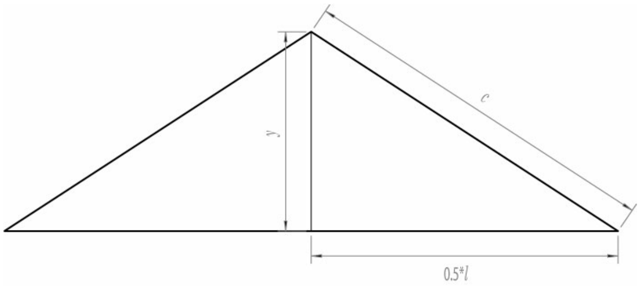

The maximum deflection:

$$y^2 = c^2 - \left(\frac{l^2}{2}\right)$$

with follows: $c = \frac{l + \Delta l}{2}$

$$y = \sqrt{\frac{(l+\Delta l)^2 - l^2}{4}} = \frac{1}{2} \cdot \sqrt{2l\Delta l + \Delta l^2} \cong \sqrt{\frac{1}{2} l\Delta l}$$

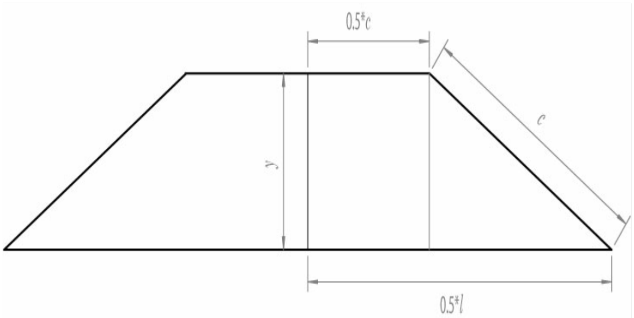

3) Approximation of deflection

$$y^2 = c^2 - \left(\frac{l-c}{2}\right)^2$$

with $c = \frac{l+\Delta l}{3}$ simplified to

$$y = \sqrt{\frac{1}{3}\left(l\Delta l + \frac{1}{4}\Delta l^2\right)} \cong \sqrt{\frac{1}{3} l\Delta l}$$

This approximation reduces the deflection by more than 18%.

4) Relationship between deflection and force

Deflection of a beam loaded with a uniform line load w and firmly clamped on both sides.

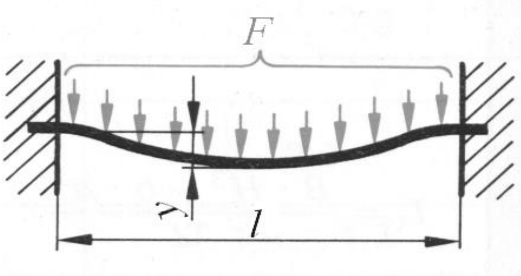

$$y = \frac{wl^4}{384EI}$$

with the area moment $I = \frac{\pi d^4}{64}$

and the line load $w = \frac{F}{l}$

$$F = \frac{6E\pi d^4}{l^3} \cdot y$$

5) Resonant frequency

The resonance frequency depends only on the geometry and the modulus of elasticity. For a beam fixed on both sides, in the 0. eigenmode (node at the clamping), without tensile stress.

$$f_{res} = \frac{22.4}{2\pi} \cdot \sqrt{\frac{EIg}{wl^4}}$$

By conversing with $w = \frac{mg}{l} = \frac{\rho\pi d^2 g}{4}$

$$f_{res} = \frac{22.4}{2\pi} \cdot \sqrt{\frac{Ed^2}{16\rho l^4}}$$

With tensile stress.

$$f_{RS} = \frac{1}{2} \cdot \sqrt{\frac{Tg}{wl^4}}$$

4.2.2 Deflection due to bending

A bending moment acts on the excessive proportion of the wire on a bent wire.

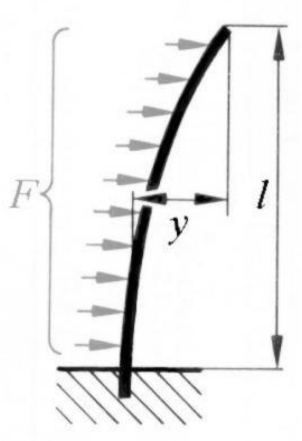

1) Maximum permissible bending load

$$\sigma = \frac{M}{W}$$

With the axial resistance torque $W = \frac{I}{r} = \frac{\pi d^3}{32}$

and the torque $M = \frac{1}{2} F_b h = \frac{1}{2} w$, the following result is obtained

$$F_b = \frac{\sigma \pi d^3}{16h}$$

2) Deflection due to bending stress

$$y = \frac{w_b h^4}{8EI}$$

By forming:

$$F_b = \frac{E \pi d^4}{8h^3} \cdot y$$

$$w_b = w_l \frac{h}{l}$$

$$F = \frac{E \pi d^4 l}{8h^4} \cdot y$$

3) resonant frequency

$$f_{res} = \frac{3.52}{2\pi} \sqrt{\frac{EIg}{wl^4}}$$

with $w = \frac{mg}{l} = \frac{\rho \pi d^2 g}{4}$ and $I = \frac{\pi d^4}{64}$ folllows

$$f_{res} = \frac{3.52}{2\pi} \cdot \sqrt{\frac{Ed^2}{16\rho l^4}}$$

The share of the bending in the total deflection is, with the usual designs, so small that it can remain unconsidered in the rough calculation.

4.2.3 Deflection due to torsion

The ignition wires are not installed as straight beams, but bent. Thus a torque is generated when the force is applied. This depends to a large extent on the design. Sometimes it is difficult to determine the proportion of the wire that is twisted.

1) Maximum deflection

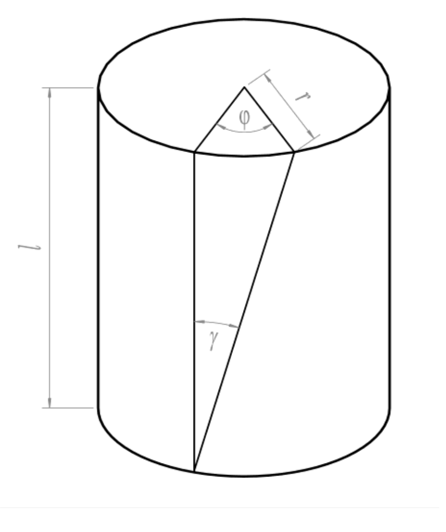

The definition of torsional stress applies analogously to tensile stress.

Hook's law of torsion:

$$\tau = G\gamma \;;\; G = \frac{\tau}{\gamma}$$

with $r\varphi = b$ and small angle approximation results in

$$\gamma \cong \frac{r}{l_T}\varphi$$

from this:

$\tau \cong G\dfrac{r}{l_T}\varphi$ follows.

The torsional stress τ and the shear modulus G move, depending on the material, at the following intervals

$\dfrac{E}{2} < G < \dfrac{E}{3}$ and . $0.57 < \sigma < 0.7$

The rule of thumb in materials engineering is:

$G = \dfrac{1}{3}E$ and $\tau = 0.7\sigma$

thus the angle at which the permissible torsional stress is reached can be calculated.

$$\varphi = 2.1 \cdot \frac{\sigma\ l_T}{Er}$$

2) Force as a function of deflection

The following applies to the effective torque

$$\tau = \frac{M}{W_P}$$

The point of application of the resulting force is at a uniform line load

$$s_T = \frac{1}{2}h$$

If this is inserted into the Hook torsion equation, the following results

$$F_T = \frac{\varphi}{\cos\varphi} \cdot \frac{2 \cdot W_P G r}{h l_T}$$

In the range of small forces, the function can be linearized, as $\cos\varphi \approx 1$ and $\varphi \approx \sin\varphi = y$.

$$F_T \approx \frac{W_p G d}{h l_T} \cdot y$$

If the polar section modulus is replaced by:

$$W_p = \frac{\pi d^3}{16}$$

so results

$$F_T \approx \frac{E\pi d^4}{48 l_T h} \cdot y$$

3) Resonant frequency

The wire behaves, below $\varphi_{0.2}$, as a torsion spring.

$$T = 2\pi\sqrt{\frac{J}{D^*}} \qquad \omega = \sqrt{\frac{D^*}{J}}$$

Calculation of spring constants

$$M_T = D^* \cdot \varphi$$

$$F_T = \frac{\varphi D^*}{\cos\varphi \cdot s_T}$$

$$D^* = \frac{\pi E d^4}{96 l_T}$$

The moment of inertia, on the other hand, can hardly be specified due to the difficult geometry.

4.2.4 Attenuation

The damping depends on the material, the grain size and its orientation, element distribution in the structure, etc. Therefore, the damping properties of the end product are determined in tests. Possible methods are, determining the logarithmic decrement or Fourier Transformation (FFT), a free decaying oscillation. It would also be conceivable to record the amplitude when driving through the frequency range in question; the superelevation and resonance frequency can be read off directly. The individual load forms overlap and influence each other. However, since neither the torsion nor the bending stress can reach critical values, the force is used as a reference for length changes. The results of
the derivations, $15mN$ can be used as a guideline for the deflecting force. The resonance frequencies are strongly dependent on the underlying model, and variate between $20kHz$ and $120kHz$.

5 EXPERIMENTAL IMPLEMENTATION

5.1 Magnet experimental setup

First, the forces were generated by means of an external magnetic field, with a current flowing through the wire.

5.1.1 Theory

An alternating current flows through the wire, which is located in a homogeneous magnetic field. The wire is deflected by the Lorentz force. The current is provided by a frequency generator with series resistor. The field is to be generated by an electromagnet and transported to the measuring point by means of a yoke.

1) Strength of the magnetic field

Force on conductor in magnetic field:

$$F = I \cdot l \cdot B$$

The size I is specified by the manufacturer or can be derived from the technical data, wire cross-section and specific conductivity.

$$B = \frac{6 y E \pi d^4}{I l^4}$$

2) Pulsed test current

With alternating currents, high peak current $\hat{I}$ values are possible if $I_{eff} = \frac{1}{T}\sqrt{\int_{t=0}^{T} i^2(t)dt}$ is observed.

But in the case of resonance, the maximum of the input energy is converted into vibration. Therefore, no increase in amplitude can be achieved by means of a pulsed test current.

3) Results

With a constant current flow, flux densities of far above $100 Tesla$ are required. When alternating current is applied, the wire can be brought into resonance, so the vibration amplitude multiplies depending on the degree of damping. Because of the relationship $B \sim y$, $B_{0.2}$ can be reduced by factor of the amplitude, if the amplitude $y_{0.2}$ is maintained.

Economic order of magnitude for magnetic fields is approx. $2 Tesla$, from $4 Tesla$ superconducting coils are necessary. At the moment 30 Tesla is the technically maximum achievable.
Experience has shown that a factor of about 100, as required here, is extremely rare, although the smallest components generally have low damping.

5.1.2 Apparatus engineering

The construction was carried out at the same time as the calculation. The observations were therefore good proof of the results of the calculations. In the first attempt a yoke was built from soft iron.

1) Dimensioning

If the strength of the maximum required flux B at the measuring point is known, the geometry of the yoke and the electromagnet can be determined from this.

$$\Theta = \sum_{k=1}^{n} H_k l_k$$

$$\Theta = I \cdot N$$

The magnetic circuit consists of $n = 3$ parts, the air gap and the yoke with constant cross-section and taper.

$$H_{luft} = \frac{B}{\mu_0}$$

$$NI = H_{joch} l_{joch} + H_{verj} l_{verj} + \frac{B l_{luft}}{\mu_0}$$

In the case of a closed, unbranched magnetic circuit with a change in cross-section, the product flux density times cross-section is constant. Since H_{joch} and H_{verj} are dependent on B, the achievable flux density must be determined by trial and error even with known geometry.

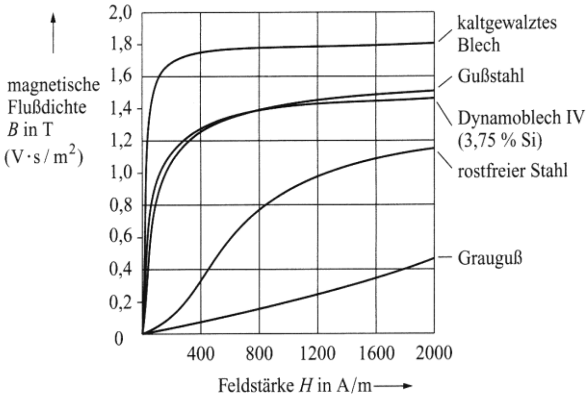

Bild 2.35 Magnetisierungskurven einiger Eisensorten

A low-alloy iron, comparable to a dynamo plate, was used. A closer look reveals that the flow is almost exclusively determined by the air gap. The limbs of the yoke and rejuvenation play a subordinate role.

$$B \approx \frac{NI\mu_0}{l_{luft}}$$

5.1.3 Bottom line

For

$$N = 190 \; I = 15A \; l_{luft} \cong 15mm$$

the flux density in the parenthesis results in

$$B \approx 350mT$$

This value is slightly higher than the one given in the construction. No movement of the wire could be observed.

5.2 Electrostatic conversion

5.2.1 Basics

The wire is to be attracted by an oppositely charged, comparatively large metal plate.
The following equations are used:

$$F = QE$$

$$\frac{F}{A} = \frac{Q}{A} \cdot E = DE$$

with $D = \varepsilon_0 \varepsilon_r E$ follows:

$$\frac{F}{A} = \varepsilon_0 \varepsilon_r E^2$$

The force therefore increases quadratically with the field strength. Due to the small radius of curvature of the wire, the field here becomes very dense. The probability of ignition decreases with a very small surface. It is assumed that the small number of surrounding gas molecules makes ionization less likely.

1) Achievable field strengths

There are no unambiguous laws, but empirical data on the breakdown behaviour of differently shaped electrodes under various pressures and atmospheres have been determined. The relationship between conductor radius and dielectric strength at high pressures in the cylinder field is as follows:

$E_{rz} = A\delta\left(1+\frac{B}{\sqrt{\delta \cdot r}}\right)$ with $\delta = \frac{Tatsächlicher\_Druck}{Normdruck}$

The investigations that led to this regularity were carried out with wire thicknesses from 0.1 to 30 cm. Depending on the polarity and ambient medium, the specifications of the parameters A and B. They are given as an average with $A = 30.3$ and $B = 0.3$.
The polarity of the electrodes also plays a role in the strength, so a higher field strength can be expected with negative wire at high pressure and small radius. The maximum field strength is reached with corona formation, a further increase of the applied voltage leads only to an enlargement of the corona. Since the ionized atmosphere in the corona is highly reactive, corona formation should be avoided during material testing.

2) Field strength on wire

In gas atmosphere with $\varepsilon_r = 1$

$$E = \sqrt{\frac{F}{A\varepsilon_0}}$$

A is the surface portion of the wire that causes the attracting force.

3) Voltage at the electrodes

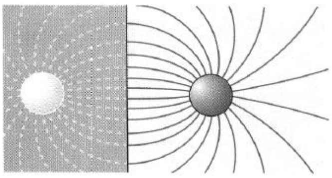

The field lines between a cylindrical conductor and a large flat counter-electrode have the same course as with a cylindrical counter-electrode at twice the distance. The flat electrode behaves like a mirror.

The field strength at the cylinder surface as a function of the voltage

$$E = \frac{U\sqrt{\left(\frac{c}{2r}\right)^2 - 1}}{(c-2r)\ln\left[\frac{c}{2r} + \sqrt{\left(\frac{c}{2r}\right)^2 - 1}\right]}$$ with c =axis distance

If the axis distance is very large compared to the radius, the formula changes to:

$$E = \frac{U}{2r\ln\left(\frac{c}{r}\right)}$$

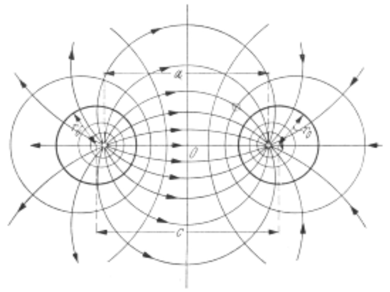

Abb.11.14. Potentiallinien und Verschiebungslinien der parallelen Linienquellen entgegengesetzt gleicher Ladung

If the mean potential area is replaced by an electrode again, the voltage is half as high as between the cylinders with the same charge of the cylinder and thus the same field strength.

$$U = Er\ln\left(\frac{2a}{r}\right)$$

$$2a = c$$

5.2.2 Setup

1) Pressure vessel

The material should have a high dielectric strength and also be stiff to withstand the mechanical loads that occur. The choice fell on PMMA (acrylic glass) because it is on the one hand transparent and thus enables observation of the wire, on the other hand it is a very stiff plastic. A dielectric constant of 2 to 3 cannot generally be avoided with plastics, so a change in the field must already be expected by the material. A further interference factor are the supply line pins in the igniter and the voltage supply of the igniter.

2) Dimensioning

Initially the idea was to operate the pressure vessel with different gases. In the case of nitrogen or carbon dioxide, pressures of up to $30bar$ would be necessarly required to achieve a high dielectric strength. A quadruple safety was included in the calculation. This resulted in a cylinder of min $100mm$ diameter with a centre bore of $16mm$ diameter. In this bore a viewing window (thickness $25mm$, also made of PMMA) was screwed from above and a holder for the igniter from below. The electrodes were screwed in from the opposite sides of the cylinder in order to apply the force alternately if necessary. An external seal allowed the geometry of the electrode to be arbitrarily shaped inside. A large-area electrode (diameter 8 mm) with rounded edges and a very thin electrode (head diameter approx. 0.5 mm) were fabricated. The choice later fell on strongly electronegative gases such as freon or sulfur hexaflouride, since high dielectric strength can be achieved with little effort. Special pressure valves would have been necessary for the partly high pressures of the other gases.

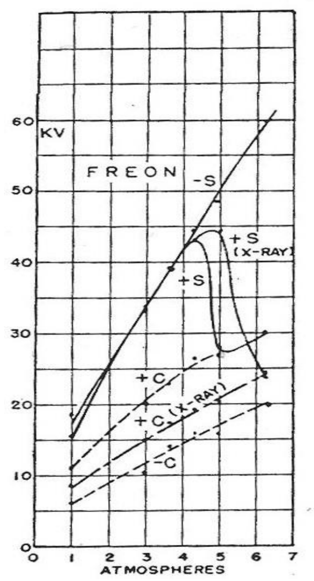

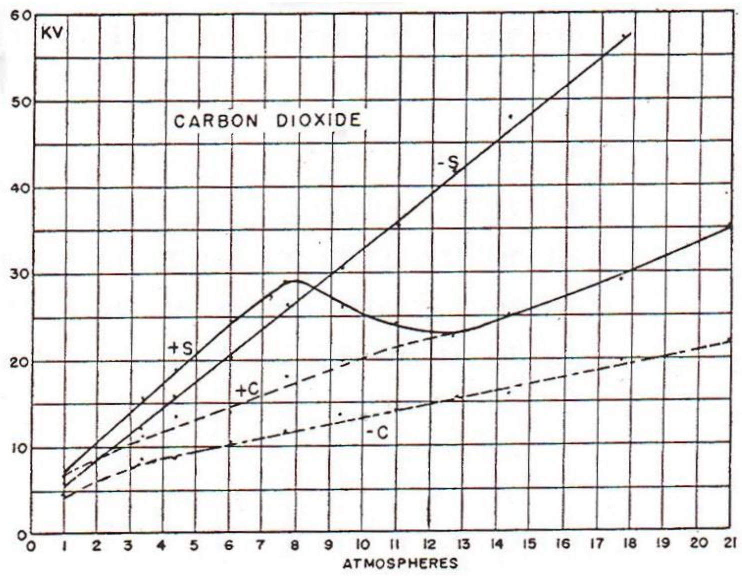

3) Results

The test setup was wired differently. The sample chamber was filled with Freon. A pressure of $5bar$ has proved to be optimal in preliminary tests. At higher pressures until $6bar$, the dielectric strength increased only insignificantly and corona formation was not observed.

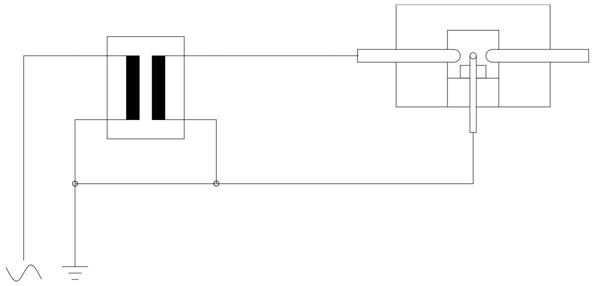

Transformer with $U = 5{,}7kV_{RMS}$ bei $50Hz$ connected to one electrode. For the large electrode, the distance to the wire was approximately for $2mm$ the thin electrode, approximately $1mm$. With this construction neither a movement of the wire nor a breakdown could be produced. The performance of the second structure was increased.

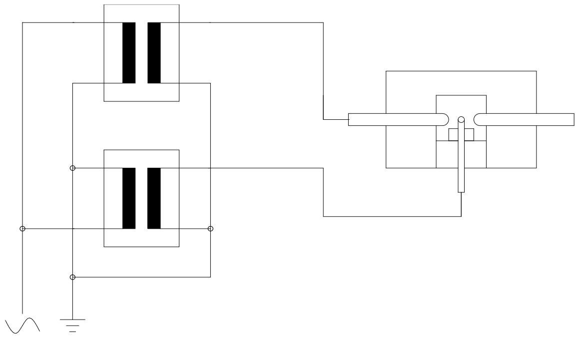

Here, two transformers, on wire and large electrode (distance $\approx 1mm$), work in phase opposition, whereby the peak voltage is increased $U = 11{,}5kV_{RMS}$ to. It can be used with this circuit without prior notice, by corona formation, during $U \approx 9kV_{RMS}$ discharge. Also here no movement of the wire could be observed before the discharge.

Conditions for the third circuit were a further increase in dielectric strength and a better detection of the corona.

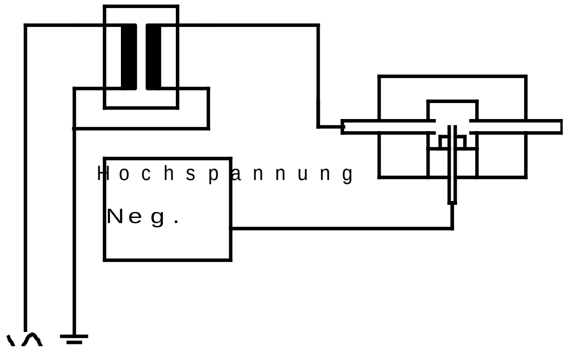

The electrode was connected to the transformer. The electrode is put on negative potential, that applies: $\hat{U}_{Trafo} \cong U_{Draht}$.

The idea was that in a system, large area against a spike (location of high curvature in space), the discharge at negative spike to positive area occurs only at higher voltages than at reverse polarization. Since the wire is also a strongly curved place, the voltages could be brought up to $U = 10kV_{RMS}$ with the thin electrode at a distance of to $\approx 0{,}5mm$ the wire. The large electrode no longer produced a breakthrough. A movement of the wire could still not be observed.

4) Further considerations

With the small electrode it always came unpredictably to a break-through, no luminous phenomena could be observed, neither in the darkened area. With the large-area electrode, a weak corona formation in the form of small light points could be seen. The locations of these discharges were on the outer edges of the pins, not the wire. This did not change until the breakthrough of the electrode, so it can be assumed that the wire is shielded from the electric field by the pins. In order to reduce the shielding, a 10-times enlarged model was used (the pins remained slightly smaller in proportion). In this way, the electrode could be attached directly to the wire, so to speak flatly between the pins. The wire could be set into vibration without any problems, which confirmed the functional principle.
However, a miniaturization on the real case seemed to be too uncertain and difficult to realize.

5.3 Influx

After the implementation attempts over electromagnetic fields, now the idea came on to excite the wire nevertheless directly mechanically. A fixed finger was not used for force transmission, as possible damage to the wire cannot be ruled out. If you let the carrier become softer and softer in your mind, you will get a jelly or a liquid which could not be damaging the wire. The transmitted force cannot be calculated due to the complex flow dynamics. For the estimation a completely turbulent flow behind the wire was assumed. The following applies here:

$$F_w = c_w A_T \frac{\rho}{2} V^2$$

One would be dependent on a permanent observation of the deformations on the wire, from which the internal tensions can be derived.

5.3.1 Flow channel with fluid

High density liquids can generate a high force even at low flow velocities. Most of them behave similarly to Newtonian fluids, so the flow velocity at the surface is zero and increases with distance depending on viscosity.

The velocity distribution in a channel

$$V_{(R)} = \frac{\Delta p}{4\eta l} \cdot \left(R^2 - r^2\right)$$

R is the pipe diameter and r the observation location.

Examples of viscosities:

$\eta_{Wasser} = 1{,}0 \cdot 10^{-3}$ (at 20°C)

$\eta_{Motoröl} \approx 400 \cdot 10^{-3}$ (depending on type)

The ignition wires are often installed close to the surfaces, resulting in low flow velocities and thus low forces. Due to the good density/viscosity ratio, degassed water was used for the tests. Oils have a lower density and because of their higher viscosity a lower flow velocity at the same pressure, thus a lower interaction with the wire.

The flow channel consisted of a narrow tube with a transparent lid, the cross-sectional area was $10mm^2$. The igniter was inserted from below, the connection terminals for the pump and the expansion tank are located on the sides.

In the first implementation, a diaphragm pump ensured the movement of the liquid. The flow velocities were not sufficient to produce a visible effect on the wire. As the pump was already working at its capacity limit, a narrowing of the canal cross-section was out of the question. The second implementation then worked with a pneumatic piston, driven by an eccentric disc. This provided sufficient working volume and pressure.

Multiple steel-coated pneumatic hoses were used for the connections in order to avoid pressure losses.

In spite of the use of pneumatic high pressure parts, gas bubbles always came into the interior of the body, which remained even after the switch-off, i.e. were not caused by cavitation. Probably the limits of the sealing materials were reached, probably in the piston. A further increase of the flow velocity was therefore no longer possible.

5.3.2 Air

Air could be regarded as the extreme case of fluid conversion in terms of viscosity. Air can easily be directed through small nozzles to the exact destination. High forces can be generated by such a strong bundling. But high turbulence leads to unpredictable higher-frequency forces on the wire.

In the implementation, two opposing nozzles, slightly offset in height, were attached to a movable plate. Moved up and down by a drive, the compressed air now hit the intermediate wire alternately. The nozzles had an inside diameter of $0{,}5mm$ and a distance from the wire of $1-2mm$. The in house compressor was used as a constand $6bar$ compressed air supply.

For the first time, this last attempt at implementation led to an ignition wire being destroyed by applied vibrations. However, a completely statistical distribution of the lifespan of the wire was found in further runs. At $400\,U/\min$ and above settings, the service life ranged from 30s to over an hour.

Fuse no.	1	2	3	4	5	6	7	8	9	10
Duration in min:sec	0:50	27:30	1:40	∞	4:40	26:20	∞	15:30	10:30	7:30
Change	700	22000	1400	-	3800	21000	-	12400	8400	6000

Fuse no.	11	12	13	14	15	16	17	18
Duration in min:sec	∞	0:30	5:40	13:50	3:50	25:20	8:00	18:50
Change	-	400	4500	11000	3100	20000	6400	15000

∞ : means a service life of more than one hour

A closer examination of the reproducibility was no longer carried out.

6 FINAL THOUGHT

The fact that no tests have yet been designed on this microtechnological topic is not surprising given the complex problems involved. Under the condition of examining the component as contactlessly as possible due to its sensitivity, there are hardly any possibilities of allowing sufficient forces to act.

With electric and magnetic fields, the test object must be electrically conductive from the outset. This is an obstacle in terms of wider application, outside the testing of airbag igniters. In addition, the interactions with the fields are too low to develop a test procedure on this basis, if the effort required for a student research project is reasonable.
The implementation by the flow of the wire led, under the realized test conditions, to first results. A continuation should be built on this insight.

Dr. Julius Nickl
Author and
internal audit

7 APPENDIX

Bibliography

Gänger, B. (1953). The electrical breakdown of gases

Gomeringer, R. et al. (2019). Table book metal: with formulary

Krause, K. Basics of electrical engineering. www.weblearn.hs-bremen.de

Lindner, H. et al. (1998). Pocketbook of Electrical Engineering and Electronics

Miseré, F. (1934 Gas discharge at low and high frequency. *Electrical Engineering, 28(7),* 411-418.

Pollock, H.C.; Cooper, F.S. (1939). The Effect of Pressure on the Positive Point-to-Plane Discharge in N_2, O_2, CO_2, SO_2, SF_6, CCl_2F_2, Air, He and H_2 . *Physical Review, vol. 56, Issue 2,* 170-175.

Young. W. et al. (2011). Roark's Formulas for Stress and Strain

DIN 50100. (1978). Testing of Materials; Continuous Vibration Test; Definitions, Symbols, Procedure, Evaluation

EN ISO 14324. (2003). Resistance spot welding - Destructive tests of welds

8 IMAGE APPENDIX

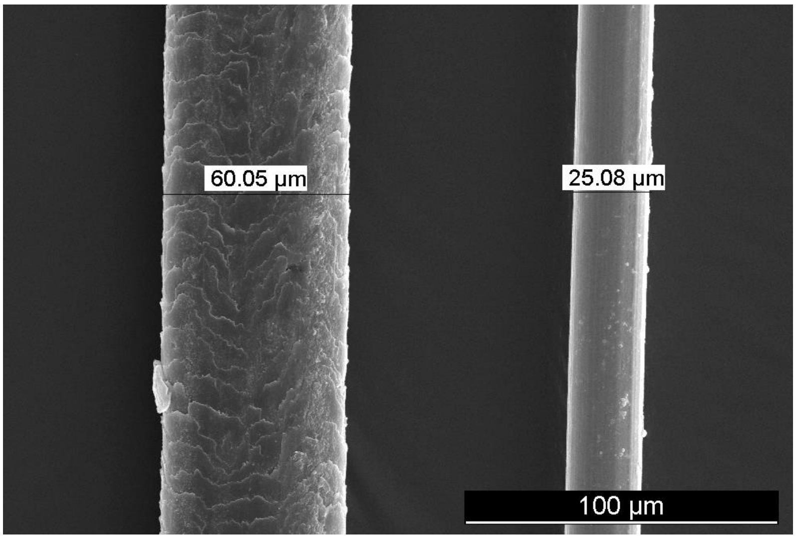

Image 1: Comparison of a human hair with a much thinner kindling wire (scanning electron microscope image).

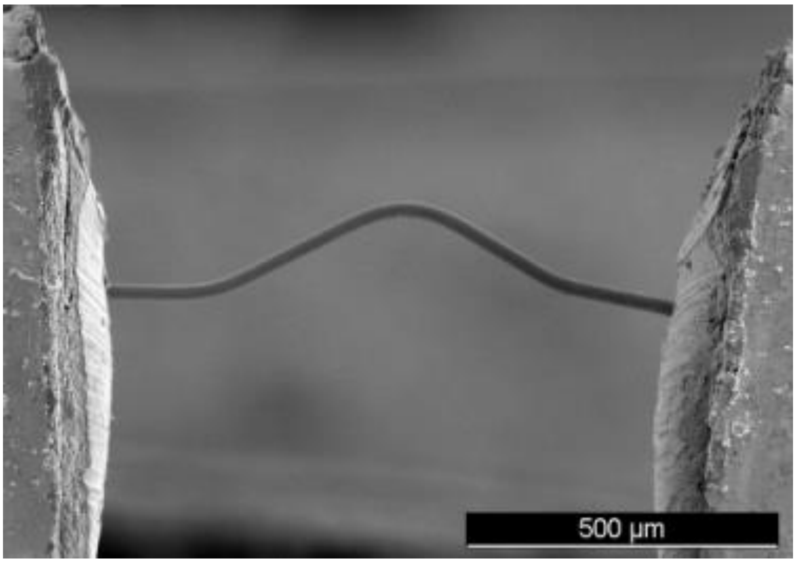

Image 2: Firing wire 100x

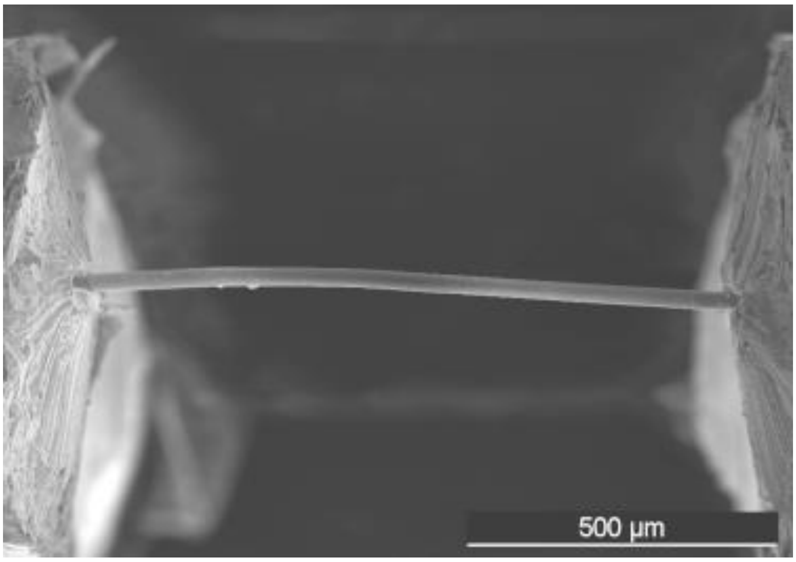

Image 3: Firing wire 100x

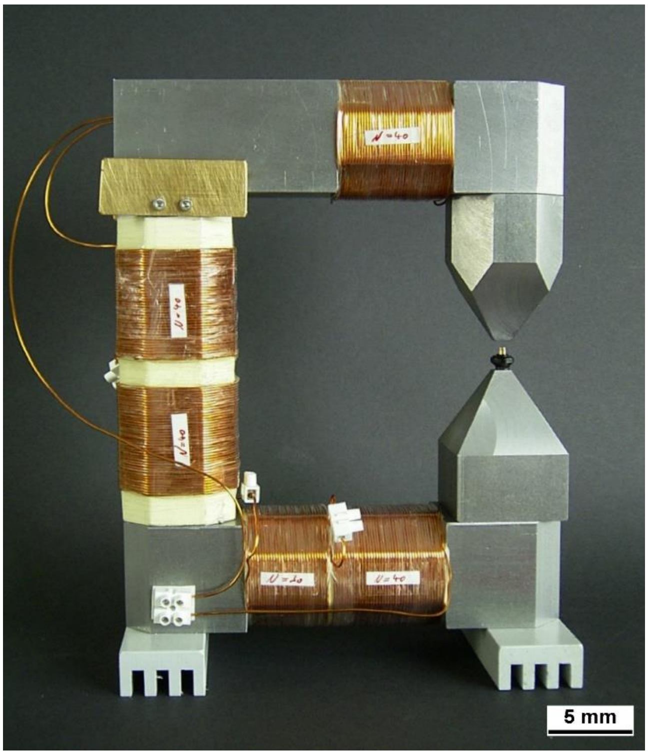

Image 4: Experimental set-up for high magnetic fields for the vibration excitation of current-carrying wires, freely suspended

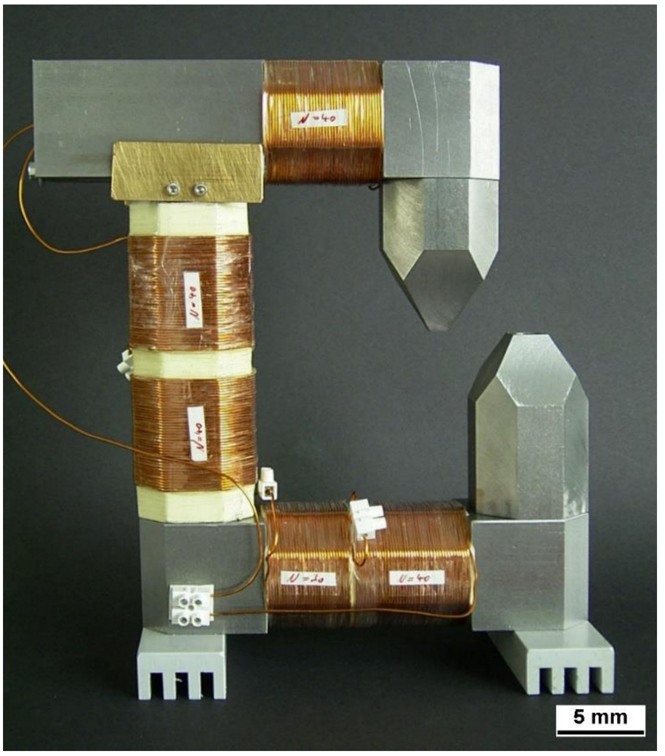

Image 5: Experimental set-up movable

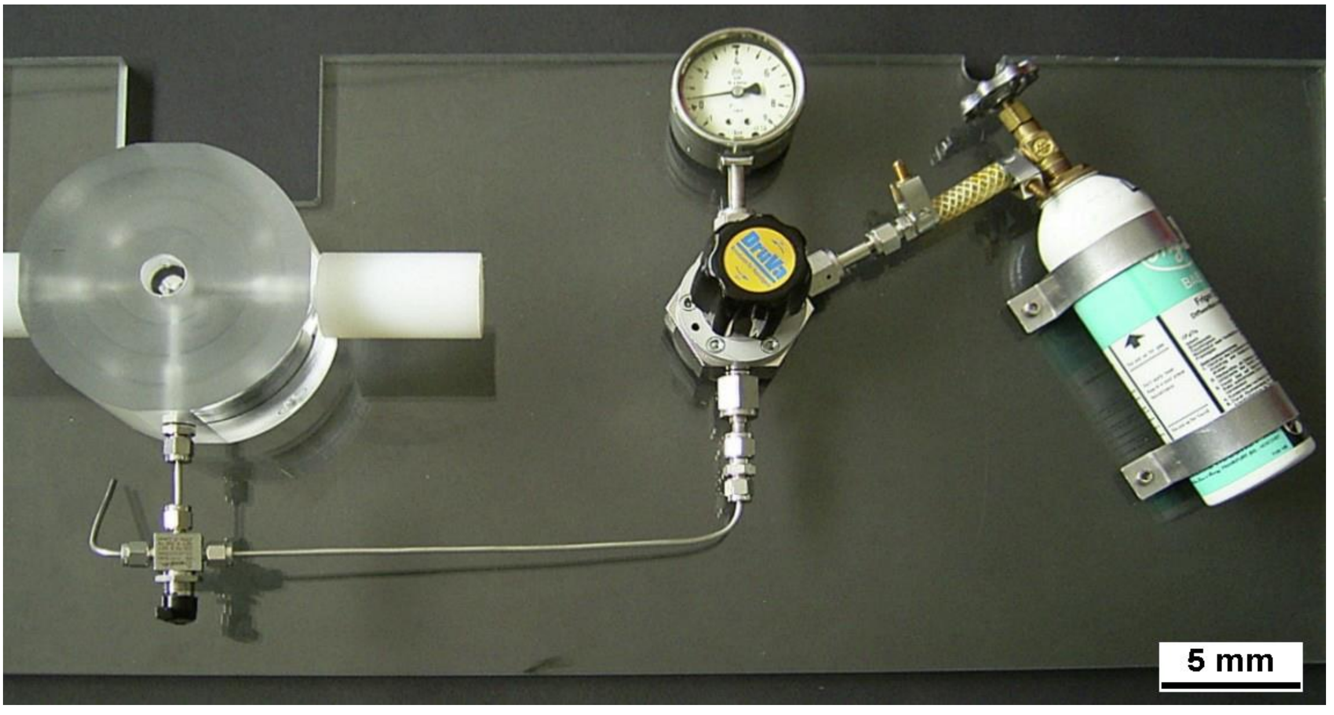

Image 6: Extinguishing gas

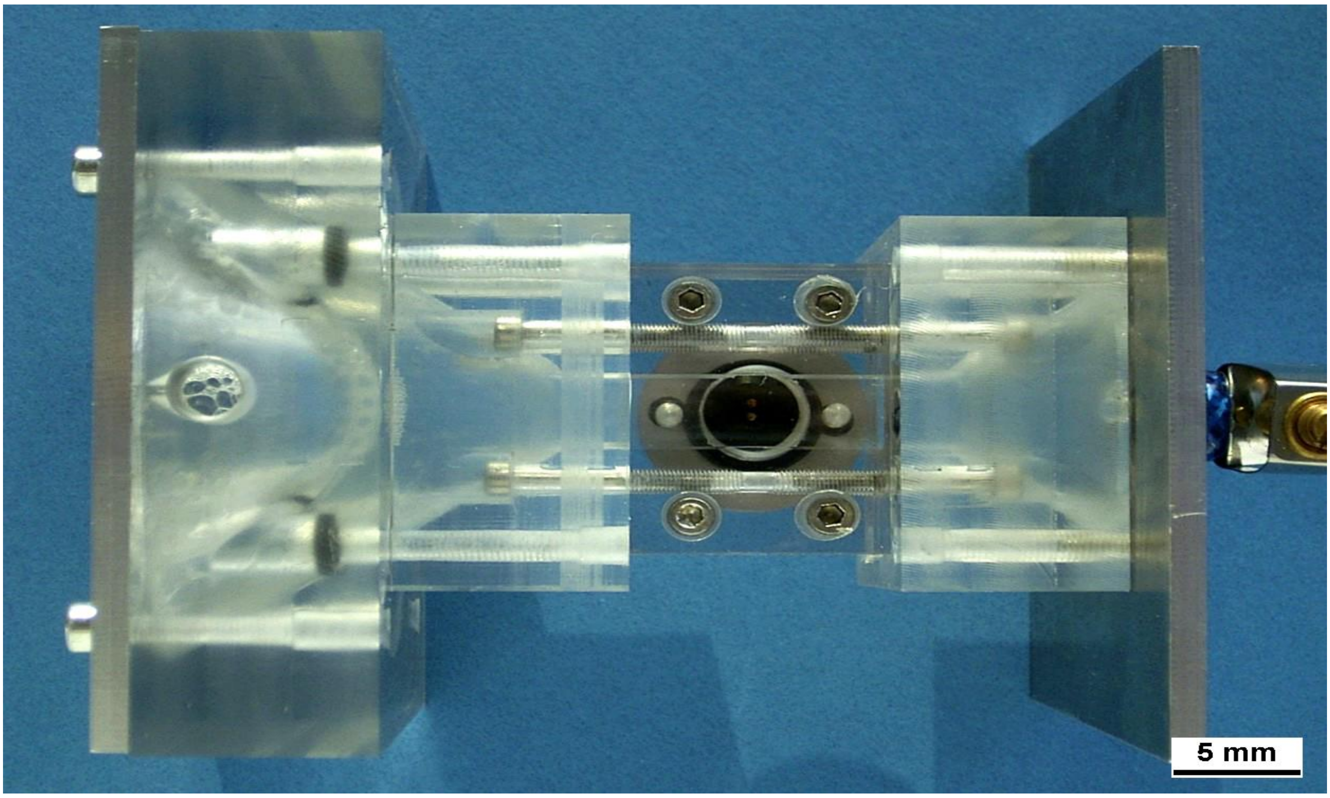

Image 7: Vibration excitation mechanical

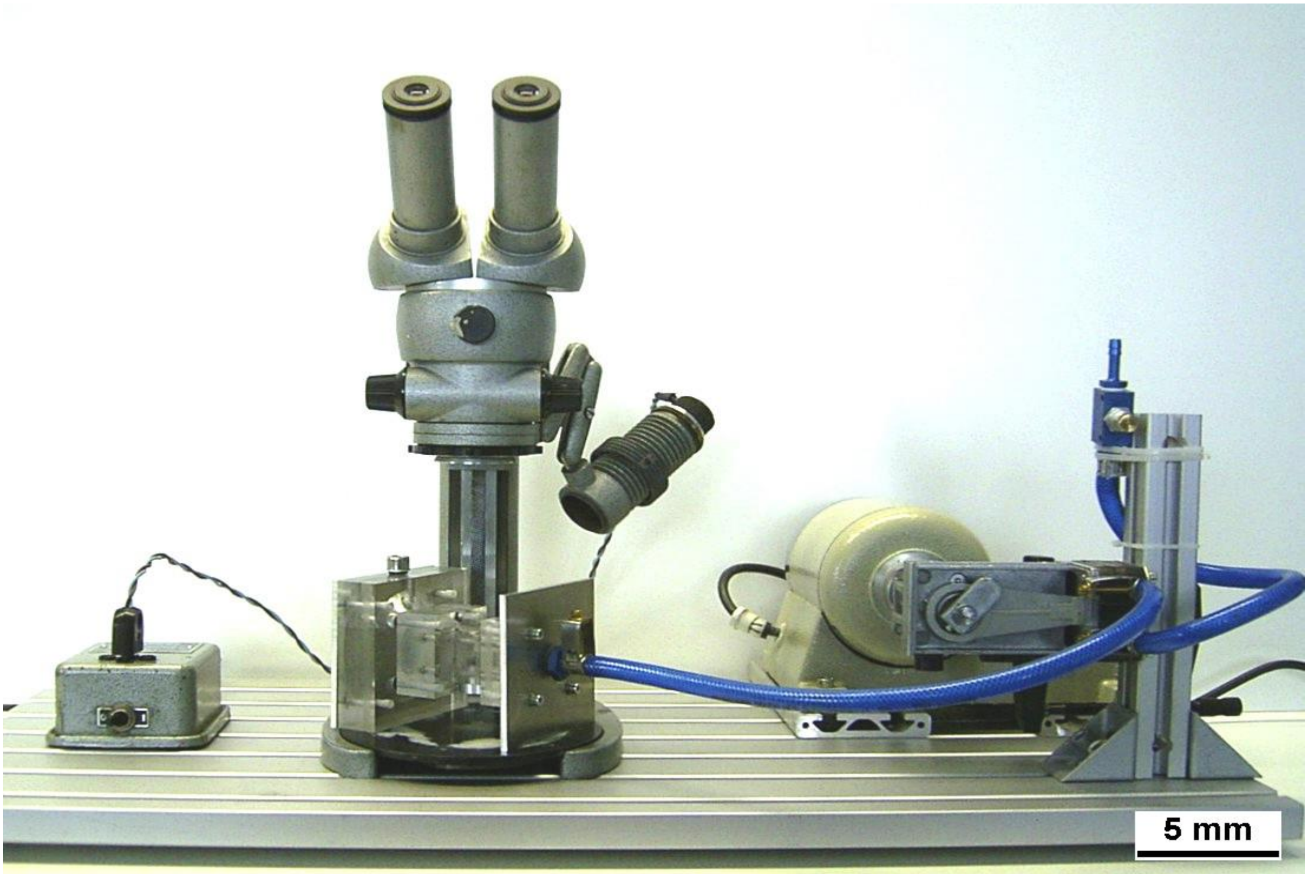

Image 8: Overall structure

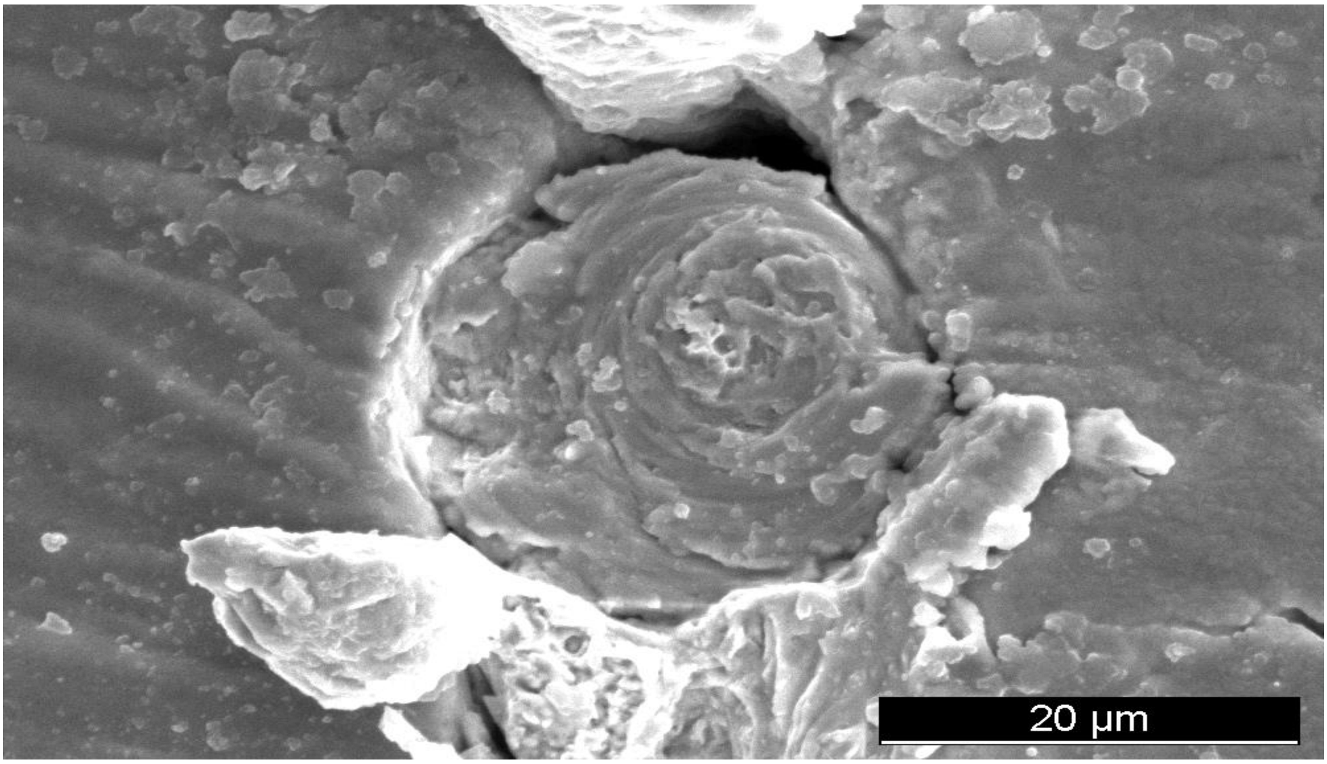

Image 10: Ring-shaped fracture pattern

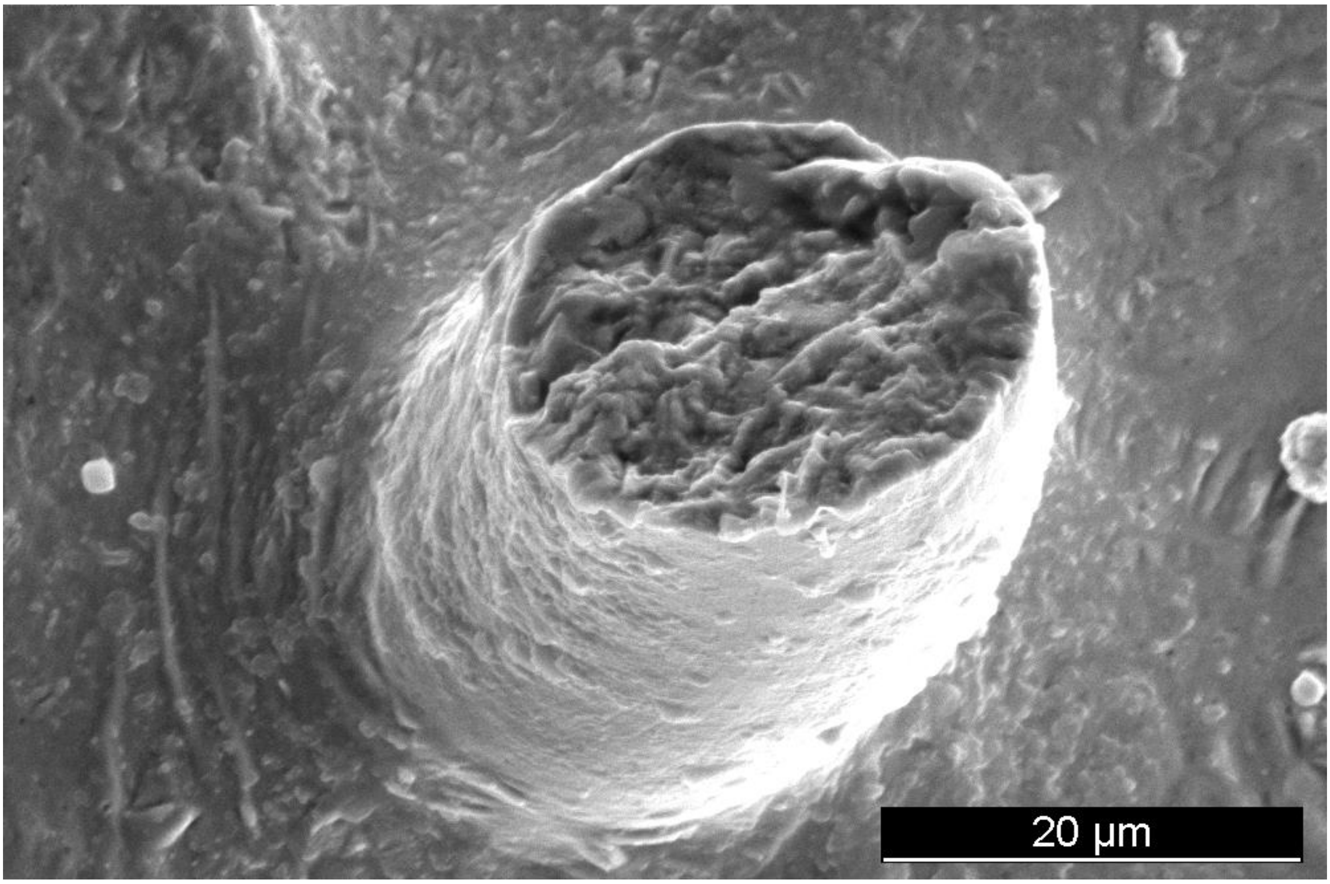

Image 9: Demolition

List of Images

9 VERSION CONTROL

Revision Date	Author	REV	Comment
2006-06-17	JAN	04	Production
2022-01-26	BeO	05	Revision new format

GWP

KNOWLEDGE CREATES PROGRESS®

- Assure quality
- Accompany developments
- Analyse damage
- Pass on knowledge

LABORATORY SERVICES

- Analytics
- Materials Testing
- Metallography
- Microscopy
- Airbag Laboratory
- Non-destructive Testing
- Physical Testing
- Fire Testing
- Workshop
- ParticleCheck
- Plastics Laboratory
- Environmental Simulation
- Explosives Laboratory

DAMAGE ANALYSIS & DEVELOPMENT SUPPORT

- Airbag
- Automotive
- Plastics
- Catalysis
- Batteries
- Construction Industry
- Chemistry
- Electrical Engineering
- Mechanical Engineering
- Aviation
- Medical Technology

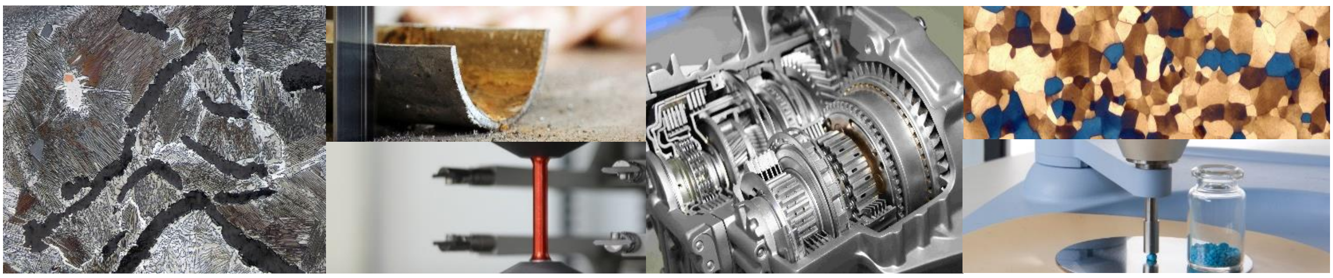

GWP - Gesellschaft für Werkstoffprüfung mbH **München | Leipzig | Saarland**
Schadensanalyse | Entwicklungsbegleitung | Labor-Services +49 (0) 8106 994 110 info@gwp.eu **www.gwp.eu**